13 June 2002

Chemical Physics Letters 359 (2002) 41–47

CHEMICAL PHYSICS LETTERS

www.elsevier.com/locate/cplett

Structure investigation of the topmost layer of a thin ordered alumina film grown on NiAl(1 1 0) by low temperature scanning tunneling microscopy

G. Ceballos, Z. Song [1], J.I. Pascual, H.-P. Rust, H. Conrad *, M. Bäumer, H.-J. Freund

Fritz-Haber-Institut der Max-Planck-Gesellschaft, Faradayweg 4-6, DE-14195 Berlin, Germany

Received 22 January 2002; in final form 4 March 2002

Abstract

A thin Al_2O_3 layer grown on NiAl(1 1 0) has been studied by scanning tunneling microscopy at about 4 K. The film exhibited monocrystalline ordering compatible with the (1 1 1) face of γ-alumina with a slightly extended surface unit cell. Although the topographical images change substantially with bias voltage we show that the autocorrelation transform of the images clearly reveals the unit cell of the alumina lattice. By using particular tunneling conditions we have identified almost all oxygen atom positions within the unit cell. The parameters applied lead to a considerable interaction between tip and top atoms of the substrate reflected in the image as local perturbations denoted as scratching.

1. Introduction

The majority of industrial applications of catalysis employ supported catalysts, which are empirically tailored to achieve the properties needed for specific reaction pathways, for instance high yield and selectivity. However, the complexity of these materials prevents the application of most surface science techniques that have been successfully used to elucidate elementary steps of some model reactions at single crystal metal surfaces [1]. In order to overcome this problem several groups started to investigate model systems comprised of monocrystalline oxide surfaces (support) with small clusters of reactive metals deposited on top (for comprehensive reviews see [2,3] and references therein). A very elegant way to avoid preparation and charging problems, which make the handling of binary oxide substrates rather difficult, has been detected by in situ formation of monocrystalline oxide films [4–6]. Thus, oxidation of the (1 1 0) surface of NiAl results in a stable well ordered film of Al_2O_3 onto which metal clusters of Rh, Pd, Pt or Cu for instance, may be deposited with tunable density and size [5,7–9]. Extended studies of this film with structure sensitive methods, like LEED,

* Corresponding author. Fax: +49-30-8413-5603.
E-mail address: conrad@fhi-berlin.mpg.de (H. Conrad).
[1] Present address: Chemistry Department, Brookhaven National Laboratory, Upton, NY 11973, USA.

0009-2614/02/$ - see front matter
PII: S0009-2614(02)00578-X

STM, ISS and ARUPS [7,8,10–14], have shown that the layer consists of two well-ordered reflexion domains with rectangular unit cells (see Fig. 1). Its thickness is about 5 Å most likely formed of two Al layers and two quasi-hexagonal oxygen layers. Various investigations as to the electronic [10,15] and chemical [10,16] properties revealed a strong resemblance to oxygen-terminated γ-Al_2O_3 with a well-defined two-dimensional band structure and a band gap very similar to that of bulk γ-alumina. A structure model based on the (1 1 1) face of γ-Al_2O_3 has been proposed [10] with a slightly extended O–O distance compared to the bulk structure.

Despite the bulk of data collected about the alumina film grown on NiAl(1 1 0) and the subsequent studies characterizing the electronic and chemical properties of metallic cluster deposited on top, up to now it had not been possible to establish a detailed structure model of the atomic positions of oxygen in the terminating layer. The large size of the surface unit cell prohibits a definite assignment by dynamic LEED investigations [13]. Also STM studies [7,8,13] had not able so far to identify the geometric positions within the unit cell because of the huge band gap of the oxide. The images obtained for different bias voltages thus vary substantially and it is not clear if the apparent structures are from the top layer or the region in between the top and interface layer. However, by tuning the bias voltage in such a way that the STM image should be dominated by contributions from the interface, it had been possible to propose a structure model, which describes the distortion of the topmost NiAl(1 1 0) layer as induced by the covering alumina film [13]. Elaborate DFT slab calculations have been performed to elucidate structure and interface of a thin alumina film on top of a metallic substrate. Even though the substrates used there did not include NiAl(1 1 0) because of the complexity caused by the symmetry domains, a chemisorbed layer of oxygen separating substrate and alumina has been obtained and in addition a very close resemblance to κ-alumina [17]. Recently, detailed informations have been obtained with surface X-ray-diffraction experiments where also a complex structure of the interface has been found [18]. Although it was possible to identify the reflexion and the antiphase domains of the Al_2O_3 layer further details had not been ascertained. In this paper we will show that the acquisition of STM images at $\sim$4 K allows on one hand to identify the unit cell at almost every bias voltage via autocorrelation of the images. On the other hand, at very low bias voltages not only atomic resolution is achieved but also oxygen–tip interactions induced perturbations were observed in the image. By means of these features we attribute the structures in the image as due to the topmost atoms and derive a structure model of the terminating oxygen layer. It must be noticed that the terminating layer may well consist of a mixture of oxygen and Al atoms as might be enforced by the stability condition [2] at ionic surfaces. On the other hand, a strong inward relaxation of the metal ions is expected for this case as observed for instance for the Cr_2O_3(0 0 0 1) surface [19]. Thus, the results of our study remain valid.

2. Experimental

The experiments were performed in an ultra-high vacuum scanning tunneling microscope operating at $\sim$4 K. The details of the instrument have been described in a previous publication [20].

The preparation of the clean NiAl(1 1 0) substrate was done following the standard procedure by means of extended sputter–anneal cycles. The state of the resulting surface was verified by acquiring STM images at 4 K, which showed atomic resolution and a very low defect concentration [21].

The preparation of the ordered Al_2O_3 film was performed as reported in the literature [10]. Directly after the last cleaning cycle of the crystal the oxide was formed by dosing 1200 L O_2 at 550 K and annealing to 1150–1200 K for 5 min. A second oxidation treatment has been applied to fill open patches in the oxide film. All images shown were sampled at $\sim$4 K using a Pt/Ir tip.

3. Results and discussion

Based upon the previous investigations of the Al_2O_3 layer grown on the (1 1 0) surface of a NiAl

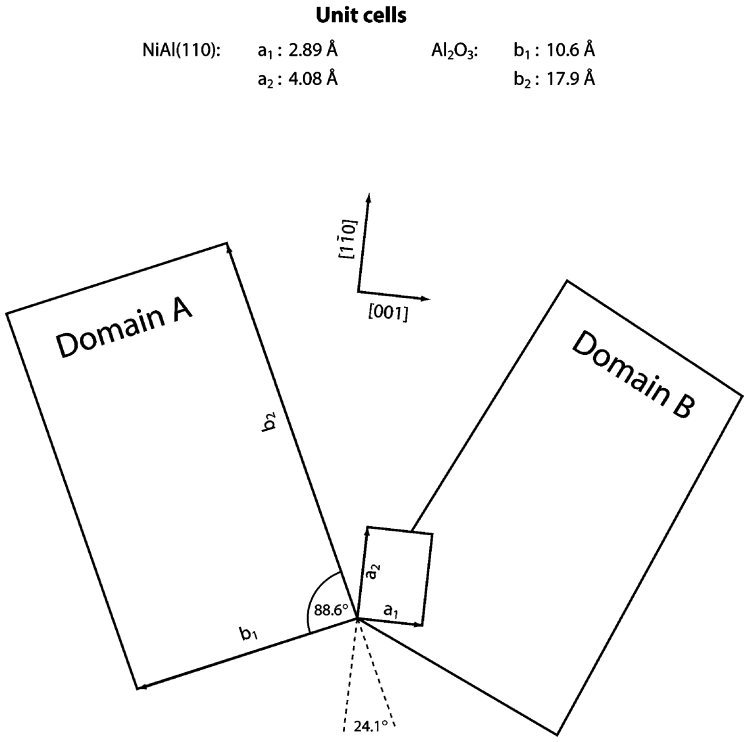

Fig. 1. Schematic drawing of size and orientation of the NiAl(1 1 1) and the Al_2O_3 unit cells (after [13]). The orientation of domain A was chosen to coincide with the unit cells derived in the STM images.

single crystal [10,13–16] size as well as orientation of the alumina unit cell with respect to the underlying NiAl lattice is well known. The schematic drawing in Fig. 1 illustrates the geometry accounting also for the two possible symmetry domains observed [10]. The phase of the monocrystalline aluminium oxide has been assigned to γ-alumina with slightly extended lattice constants (9.5% and 6.7%). It should be noted that the unit cell is not rectangular but rhomboidal with a corner angle of 88.6°.

Two STM images of the Al_2O_3 film acquired at ~4 K are displayed in Figs. 2a and b. They show the same domain of the alumina layer but are measured at a sample bias voltage of −4 V (Fig. 2a) and −1 V (Fig. 2b), respectively. It is apparent that both images exhibit a periodic arrangement but because of the very complicated intensity modulations, a quantitative determination of the constituting unit cell cannot be accomplished. In Fig. 2a a clearly regular array of elevated lines is apparent that might be identifiable with unit cell periodicities. On the other hand, a more randomly distributed number of strongly protruding spots appears to be always attached to a line thus complicating a determination of the periodicity in the other direction. The effect of such bumps is even more pronounced in Fig. 2b. When during the scan the tip approaches such a protrusion it is almost instantaneously retracted beyond the span of the *z*-piezo. Such an event is reflected by the bright spots in the image, which might be denoted as 'scratching'. Since, however, this 'scratching' does not occur in all cases, the very suggestive association of the bright spots with the Al_2O_3 lattice order is not fully convincing.

A well-established tool in image processing is the autocorrelation function. Although primarily used to detect a spatial structure of image noise or to determine the point spread function of imaging

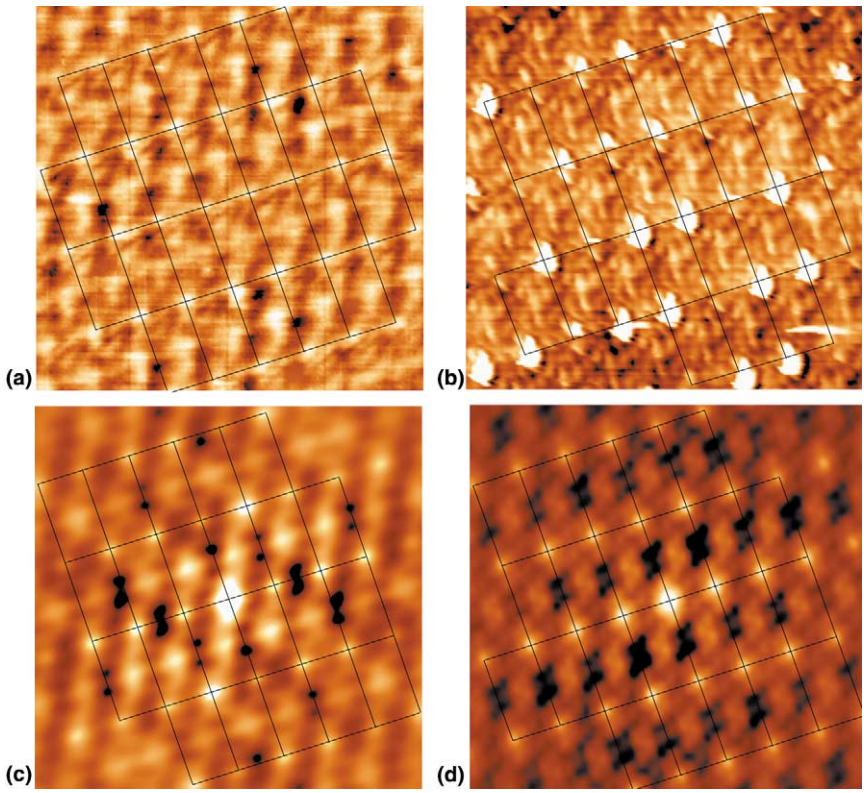

Fig. 2. STM images measured at ~4 K at the Al_2O_3 layer on NiAl(1 1 0) (a and b) with the corresponding autocorrelation images (c and d) The tunneling parameters for (a) −4 V, 4 nA, (b) −1 V, 2.6 nA. The image size is 8 × 8 nm in each image. The indicated lattice has been determined from the respective autocorrelation image and then transferred to the topographic images as one-to-one copy.

systems [22], it is also suitable for the detection of periodic structures in a complex image. The autocorrelation function is mathematically defined as

$$C(\xi,\eta) \propto \frac{1}{2X}\frac{1}{2Y}\int_{-X}^{+X}\int_{-Y}^{+Y} z(x,y) \times z(x+\xi, y+\eta)\,\mathrm{d}x\,\mathrm{d}y$$

with X and Y as the dimensions of the image matrix. In practice one uses the fluctuation $\Delta z(x,y) - \mathrm{mean}(z)$. To avoid any artificial features in the resulting matrix the image is not periodically continued but padded with zeros [22].

The autocorrelation images of Figs. 2a and b are shown in Figs. 2c and d, respectively. By convention, the point $(\xi,\eta) = (0,0)$ is located in the center of the image and the evaluation is limited to the size of the original image. Additionally, as apparent from the integral, only the upper half of the autocorrelation image contains independent information; the lower part can be constructed via a point reflection operation at the center. Also the contrast diminishes toward the image borders as the zero padded continuations of the original image come into play for the calculations.

The periodicity of the alumina layer is now obvious and the signatures of the unit cells are directly visible. Since the autocorrelation algorithm conserves the geometry it is now easy to construct for both images the corresponding lattice. The lattice thus obtained is indicated in Figs. 2c and d. The size and orientation of the respective unit cells agree perfectly within the error margins of STM. Even the deviation of the unit cell from the rectangular shape can be identified allowing

thus to locate that corner angle which is smaller than 90°. Thus, the lattice of the underlying NiAl(1 1 0) surface could in principle be constructed as well on basis of the schematics in Fig. 1. The alumina lattice as determined from the autocorrelation pictures is then transferred directly to the STM images. Its absolute position within the images is obviously undetermined, and we chose as corner locations the maximum overlap with the respective brightest spots. The repetitive character of structural details within each unit cell is now easily identified although the visibility of the individual shapes varies considerably, as is typical for STM images.

Closer inspection of Figs. 2a and b reveals that the distinctness of the fine structures within the respective unit cells varies substantially. The shapes in the higher bias image (Fig. 2a) appear very fuzzy impeding thus an identification of particular atom positions. Although the details in Fig. 2b are much better resolved a reliable allocation of individual position is not possible. Apart from protruding features at each unit cell center no similarities between the two images can be convincingly specified. Moreover, no resemblance to the configuration of the oxygen terminated γ-Al_2O_3(1 1 1) surface is found, which is expected from the previous studies and proposed in [10].

On the other hand, the effect observed here, namely the improvement of resolution upon bias voltage reduction, has been recognized before [13] but the reason of which could not be identified yet. Following this empirical evidence, we acquired an image at a sample bias voltage of −100 mV. The current was set to such a value that the 'scratching' described above just sets in. Fig. 3a shows the resulting image. It is apparent that in addition to the arrangement of circular features (note the very bright regular pairs) a periodic pattern of structures exists that is clearly due to 'scratching'. Moreover, some stripes are evident which are typical for a contact of the tip, particularly visible in the lower right corner of Fig. 3a. As in Figs. 2a and b autocorrelation is used to extract the surface unit cell. The resulting image is shown in Fig. 3b. The periodicity of the STM image is here particularly evident and the derived lattice is superimposed onto the autocorrelation image. A naive

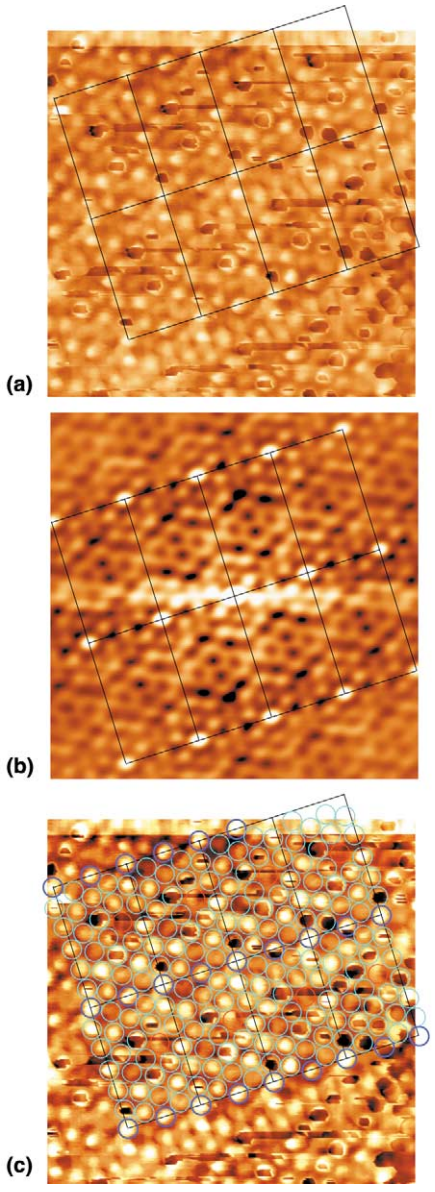

Fig. 3. STM image measured at ~4 K with a sample bias voltage of −100 mV and a current of 4 nA (a). The size is 4.8 × 4.8 nm. Part (b) shows the corresponding autocorrelation image with the alumina lattice. The lattice indicated in (a) is a one-to-one copy of the such determined lattice. Part (c) displays again the topographic image but with the featured emphasized by unsharp masking of the original. Additionally, the circles drawn in (c) correspond to the positions of the oxygen atoms derived as described in the text.

transfer of this lattice to the original image is again indeterminate since the choice of the lattice corners is arbitrary. It would be tempting to retrieve the pattern of the autocorrelation image in the STM image but the high symmetry of the former is naturally not present in the latter as it is artificially created by the autocorrelation formalism. The position decided for and shown in Fig. 3a is to some extent an attempt to recover part of the features close to the $(\xi, \eta) = (0, 0)$ position of Fig. 3b.

It is, however, likely to identify the round structures in the STM image with the oxygen atoms in the terminating layer, and to determine their location within the unit cell. This positioning has been performed by pinpointing with circles all visible protrusions in the upper left unit cell. Subsequently, this sample arrangement has been shifted along the lattice vectors permitting thus a better identification and positioning of all periodic features by way of averaging by eye. The so obtained oxygen atom locations are displayed in Fig. 3c on top of the STM image, which has been filtered by unsharp masking to emphasize the bright features.

A closer inspection of the oxygen positions in Fig. 3c reveals that no symmetry order can be detected inside a unit cell. On the contrary, the location of the oxygen atoms seems to be rather arbitrary. However, a remnant of a hexagonal symmetry traced back to the γ-alumina (1 1 1) face can be detected in form of distorted hexagonal pattern. This is in accord with previous LEED investigations [10,13] where an approximate hexagonal pattern has been observed but with streaky intensities along a ring centered at the $(0, 0)$ reflex. The distortion of the (1 1 1) symmetry is obviously be due to the mismatch between the NiAl(1 1 0) substrate and the alumina film accounted for by the slight extension of the Al_2O_3 lattice [10].

The question still to be discussed is connected with the electronic structure of the alumina film. In the previous ARUPS studies [10] the large band gap of about 8 eV characteristic for Al_2O_3 has been also observed for the thin film on NiAl(1 1 0). In consequence, there should be no electronic states in the film into which the electrons from or to the tip can tunnel, below a sample bias voltage of 4 V. Only by tunneling through the alumina layer also, electron states in the NiAl substrate should be available. In that case, topographic images should reflect the geometry of the interface [13]. To explain the quite contrasting experimental data observed here, we propose the following picture: for low bias voltages as used for the STM image in Fig. 3, the tip–surface distance is so small that the tunneling event has to be considered as a totally localized process thus overriding any periodicity of the surface which is the origin of the band gap description. Moreover, at this distance the tip–surface interaction cannot be neglected and it is likely to assume that this interaction might induce localized electronic states at the oxygen atoms from which the electrons can tunnel. If the distance becomes too small this interaction might even affect the position of the surface atoms, leading to the above mentioned 'scratching' that is abundant in Fig. 3. Such a kind of accounting for the interaction between surface and tip forms naturally the core of understanding of the results of atomic force microscopy in both the contact and the non-contact mode. Moreover, all theoretical approaches to tunneling microscopy involve the local character of the processes in conjunction with chemical interactions between tip and substrate, in particular for small distances. A recent very comprehensive review of these questions from a theoretical point of view with much emphasis on AFM is found in [23]. Additionally, a survey of STM at semiconductor surfaces combining theoretical and experimental aspects has also been published recently [24].

On the other hand, at higher bias voltages the tunneling through the isolating alumina layer may be considered in terms of scattering at an array of repulsive potentials being due to the negatively charged oxygen ions. In consequence, the apparent 'topographical' STM image contains information sampled over the height of the alumina film, and it is not surprising that a reasonable structure determination is not possible, in particular if the strong energy dependence of potential scattering is considered.

In summary, by imaging the well-ordered Al_2O_3 layer with a low temperature STM we were able to determine the surface unit cell at several bias

voltages by using the autocorrelation transform. At specific tunneling conditions atomic resolution of the terminating oxygen layer was achieved allowing the determination of individual atom positions within the alumina unit cell. The tunneling mode employed apparently leads to a considerable interaction between the tip and the top oxygen atoms thus overcoming the electronic barrier of the band gap of the isolating film. The effect has been tentatively attributed to the formation of electronic states locally created by the tip–substrate interaction.

Acknowledgements

We thank K. Weiss for vivid discussions, M. Heemeier and M. Frank for their help with the alumina film preparation. Z.S. thanks the scholarship from the agreement between Max-Planck-Gesellschaft and Chinese Academy of Science. J.I.P. is indebted to the European Union for his grant under the Marie Curie scheme.

References

[1] C.B. Duke (Ed.), Surface Science: The First Thirty Years, Elsevier, Amsterdam, 1994;
D.A. King, D.P. Woodruff (Eds.), The Chemical Physics of Solid Surfaces and Heterogeneous Catalysis, vols. 1–9, Elsevier, Amsterdam, 1982–2001.
[2] H.-J. Freund, Farad. Disc. 114 (1999) 1.
[3] C.T. Campbell, Surf. Sci. Rep. 27 (1997) 1.
[4] S. Street, C. Xu, D. Goodman, Annu. Rev. Phys. Chem. 48 (1997) 43.
[5] M. Bäumer, H.-J. Freund, Progr. Surf. Sci. 61 (1999) 12.
[6] R. Franchy, Surf. Sci. Rep. 38 (2000) 195.
[7] K. Højrup Hansen, T. Worren, S. Stempel, E. Lægsgaard, M. Bäumer, F. Besenbacher, I. Stensgaard, Phys. Rev. Lett. 83 (1999) 4120.
[8] T. Worren, K. Højrup Hansen, E. Lægsgaard, F. Besenbacher, I. Stensgaard, Surf. Sci. 477 (2001) 8.
[9] M. Bäumer, M. Frank, R. Kühnemuth, S. Stempel, H.-J. Freund, Surf. Sci. 454–456 (2000) 957.
[10] R.M. Jaeger, H. Kuhlenbeck, H.-J. Freund, M. Wuttig, W. Hoffmann, R. Franchy, H. Ibach, Surf. Sci. 259 (1991) 235.
[11] F. Winkelmann, S. Wohlrab, J. Libuda, M. Bäumer, D. Cappus, M. Menges, K. Al-Shamery, H. Kuhlenbeck, H.-J. Freund, Surf. Sci. 307–309 (1994) 1148.
[12] Th. Bertrams, A. Brodde, H. Neddermeyer, J. Vac. Sci. Technol. B 12 (1994) 2122.
[13] J. Libuda, F. Winkelmann, M. Bäumer, H.-J. Freund, T. Bertrams, H. Neddermeyer, K. Müller, Surf. Sci. 318 (1994) 61.
[14] J.-P. Jacobs, S. Reijne, R.J.M. Elfrink, S.N. Mikhailov, H.H. Brongersma, M. Wuttig, J. Vac. Sci. Technol. A 12 (1994) 2308.
[15] A. Sandell, J. Libuda, P. Brüwiler, S. Andersson, A. Maxwell, M. Bäumer, N. Martensson, H.-J. Freund, J. Electr. Spectr. 76 (1995) 301.
[16] R.M. Jaeger, J. Libuda, M. Bäumer, K. Homann, H. Kuhlenbeck, H.-J. Freund, J. Electr. Spectr. 64/65 (1993) 217.
[17] D.R. Jennison, C. Verdozzi, P.A. Schulzu, M.P. Sears, Phys. Rev. B 59 (1999) R15605;
D.R. Jennison, A. Bogicevic, Surf. Sci. 464 (2000) 108.
[18] A. Stierle, F. Renner, R. Streitel, H. Drosch, Phys. Rev. B 64 (2001) 165413.
[19] F. Rohr, M. Bäumer, H.-J. Freund, J.A. Mejias, V. Staemmler, S. Müller, L. Hammer, K. Heinz, Surf. Sci. 372 (1997) L291.
[20] H.-P. Rust, J. Buisset, E.K. Schweizer, L. Cramer, Rev. Sci. Instrum. 68 (1997) 129.
[21] Z. Song, J.I. Pascual, H. Conrad, K. Horn, H.-P. Rust, Appl. Phys. A 72 (2001) S159.
[22] J.C. Dainty, R. Shaw, Image Science, Academic Press, New York, 1974.
[23] D. Drakova, Rep. Progr. Phys. 64 (2001) 205.
[24] G.A.D. Briggs, A.J. Fisher, Surf. Sci. Rep. 33 (1999) 3.